

First report of a novel multiplexer pumping system coupled to a water quality probe to collect high temporal frequency in situ water chemistry measurements at multiple sites

François Birgand,*¹ Kyle Aveni-Deforge,¹ Brad Smith,² Bryan Maxwell,¹ Marc Horstman,³ Alexandra B. Gerling,⁴ Cayelan C. Carey⁴

¹Department of Biological and Agricultural Engineering, North Carolina State University, Raleigh, North Carolina

²Sungate Design Group, Raleigh, North Carolina

³WK Dickson & Co., Inc., Raleigh, North Carolina

⁴Department of Biological Sciences, Virginia Tech, Blacksburg, Virginia

Abstract

The increasing availability and use of high-frequency water quality sensors has enabled unprecedented observations of temporal variability in water chemistry in aquatic ecosystems. However, we remain limited by the prohibitive costs of these probes to explore spatial variability in natural systems. To overcome this challenge, we have developed a novel auto-sampler system that sequentially pumps water from up to 12 different sites located within a 12 m radius to a single water quality probe. This system is able to generate high temporal frequency in situ water chemistry data from multiple replicated units during experiments as well as multiple sites and depths within natural aquatic ecosystems. Thus, with one water quality probe, we are able to observe rapid changes in water chemistry concentrations over time *and* space. Here, we describe the coupled multiplexer-probe system and its performance in two case studies: a mesocosm experiment examining the effects of water current velocity on nitrogen dynamics in constructed wetland sediment cores and a whole-ecosystem manipulation of redox conditions in a reservoir. In both lotic and lentic case studies, we observed minute-scale changes in nutrient concentrations, which provide new insight on the variability of biogeochemical processes. Moreover, in the reservoir, we were able to measure rapid changes in metal concentrations, in addition to those of nutrients, in response to changes in redox. Consequently, we believe that this coupled system holds great promise for measuring biogeochemical fluxes in a diverse suite of aquatic ecosystems and experiments.

Until recently, most water quality data from aquatic ecosystems have been collected on a coarse temporal frequency, e.g., monthly, biweekly, weekly, and only rarely on daily or more frequent time scales. It is now well established that water chemistry can vary dramatically within minutes to hours in streams and rivers due to changes in flow (e.g., Chapin et al. 2004; Pellerin et al. 2009, 2011; Birgand et al. 2010), and even in lakes and reservoirs with longer residence times (e.g., Watras et al. 2015, 2016). There is emerging evidence that, even in the absence of changes in flow, there can be sizable and rapid changes in nutrient and metal concentrations likely associated with several biogeochemical processes (e.g., Nimick et al. 2011; Cohen et al. 2012, 2013; Hensley et al. 2015). However, the lack of established tools

for measuring rapid changes in water chemistry in situ represents a major challenge that has historically hindered the study of biogeochemistry at the minute scale in the aquatic environment.

New portable wet chemistry labs and optical sensors have enabled the opportunity of measuring water chemistry concentrations multiple times per hour at single monitoring stations, providing invaluable information on the temporal scale at which biogeochemical dynamics occur (e.g., Cohen et al. 2012, 2013; Etheridge et al. 2014). Given the considerable advances in our understanding of aquatic biogeochemistry gained by the deployment of high-frequency sensors at individual sites, it becomes obvious that measuring high-frequency temporal variability in water chemistry at multiple sites would likely reveal new insight on spatial heterogeneity and processes driving variability in water chemistry coupled in space and time. However, the current cost of in situ water quality probes remains a major obstacle to the concurrent

This article was published online on 29 July 2016. The authors identified that a co-author was missing. The correction was made and published on 21 September 2016.

*Correspondence: birgand@ncsu.edu

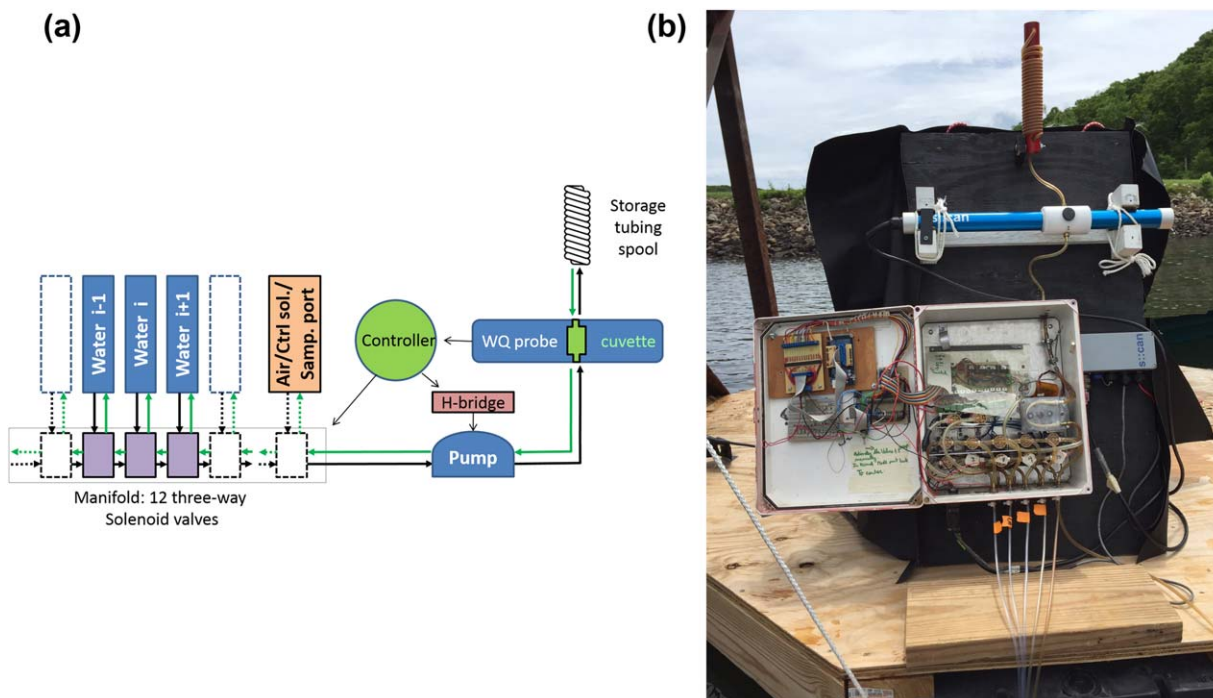


Fig. 1. (a) Schematic of the water quality probe fitted with the Multiplexer Pumping System (MPS) for the automatic and sequential measurement of water quality for up to 12 individual observation sources; (b) photograph of the MPS and probe system during deployment in the field configured to sample five distinct point sources (photo credit to C.C. Carey); the S::CAN Spectro::lyser™ water quality probe is fitted with the manufacturer's 40 mL cuvette transformed into a flow-through cell.

acquisition of both high-resolution temporal *and* spatial data.

In this article, we propose an affordable system that offers a compromise maximizing both spatial and temporal resolution for measuring water chemistry on the minute scale. We have coupled an UV-vis (Ultraviolet-visible) spectrophotometer probe with a multiplexer pumping system (MPS), which can sequentially pump water from up to 12 sources or points in space located within a limited distance of the probe, such that the temporal resolution at each of the 12 sites could be hourly at a minimum. This article describes the coupled MPS-water quality probe system, reports an evaluation of its performance, and presents two applications for wetland mesocosms and a reservoir.

Materials and procedures

Coupled MPS-water quality probe system description

Overview

To remain affordable, the system uses a single high-frequency automatic water quality probe as the central analytical instrument to which water from different sampling sites (hereafter, point sources) are pumped via a MPS (Fig. 1). Our design criteria when constructing the MPS system were: (1) to have the capacity of obtaining hourly or sub-hourly samples for measuring multiple point sources, (2) to be able to pump water from the point sources to the probe to

overcome at least 3 m of head difference, (3) to be able to run on 12 volts (V) direct current (DC) power for field deployment, and (4) that the coupled MPS-water quality probe system functioned entirely automatically. An acceptable compromise for these criteria was to design an MPS system that enabled sampling from up to 12 point source sites located within 12 m of the central probe. We note that this distance could be extended, possibly even doubled, with the appropriate tubing at the cost of reduced temporal resolution on each point source.

As the in situ field spectrophotometer can only collect one measurement at a time on fixed time intervals, we designed and built an MPS to sequentially pump and purge water from each point source to the probe, in synchrony with the probe measurements, and cycle through the sequence of measurements to obtain at least hourly time resolution of data collection at each source. To maintain the water quality probe's capability of measuring small suspended particle concentrations, we chose 3.18 mm internal diameter flexible tubing as a sampling conduit of water from the point source to the probe, fitted with 1.5 mm mesh screens at the source (although only dissolved constituent applications are shown in this article). Consequently, the coupled MPS-water quality probe system is well suited for applications where the source sampling volume is not limited and does not affect the process or system studied.

Water quality probe

The high-frequency automatic water quality probe used in our two applications was the field spectrophotometer Spectro::lyser™ (S::CAN™, Vienna, Austria). The probe has a 35 mm optical pathlength to measure nitrate, dissolved organic carbon (DOC), total organic carbon (TOC) concentrations, and turbidity from light absorbance spectra obtained from 216 wavelengths at 2.5 nm intervals between 220 nm and 737.5 nm. Several recent studies have demonstrated that the capabilities of these probes may in fact be greater than advertised as it is possible to create statistically significant correlations between additional light-absorbing and non-absorbing elements and contaminants in water (Rieger et al. 2006; Torres and Bertrand-Krajewski 2008; Etheridge et al. 2014). We report in this article the use of the probe for nitrate and additional parameters listed below.

Multiplexer pumping system overview

The seven components of the MPS include 12 in-line three-way solenoid valves and manifold, a peristaltic pump fitted with an H-bridge for current inversion, 3.18 mm polypropylene tubing, a flow-through cuvette, a storage tubing spool, and a programmable Arduino (Arduino, www.arduino.cc) micro-controller (Fig. 1). We designed the pumping system to accommodate three usage modes so that after the sensor reading, water could be (1) pumped entirely back to its source (“purge back to source”), (2) purged to a designated sampling port (“purge back to sampling port”), or (3) could be discarded (“pump/purge to discard”). The first two cases require bidirectional pumping capabilities and the presence of a storage tubing spool described herein, while in the third case, unidirectional pumping could theoretically suffice.

Solenoid valve manifold

The manifold is made of 12 in-line, three-way, 3.4 watt (W) solenoid valves (Model WTB-3R(K)-M6(14U)F—Takasago Fluidic Systems, Nagoya, Japan). In Fig. 1a, eleven valves are dedicated to different point sources and the twelfth one to a standard solution. All valves (2 mm inside diameter) are in-line with each other. Each valve’s output feeds directly into the preceding valve’s input except for the ending valve, which has its output feeding directly into the pump (Fig. 1). The inherent design of the in-line manifold implies that cross-contamination for water that is pumped through the valve furthest from the pump is potentially higher than for water pumped through the valve closest to the pump. We have devised several solutions to address this problem (see below). Valves are opened, or actuated, upon a 12 V DC signal from the controller. An important artifact of solenoid valves is that a voltage spike of > 100 V can occur when the valves are closing due to the collapse of the magnetic field existing in the solenoid. To protect the microcontroller from

this voltage surge, we installed an IRF 630 Field Effect Transistor (FET) and a 1N4007 Diode for each valve.

Peristaltic pump and H-bridge

We chose a peristaltic pump (M500, Clark Solutions™, Hudson, Massachusetts, U.S.A.) that runs on 12 V DC and consumes 12 W when pumping at maximum flow rate of 390 mL min⁻¹. A sample can be pumped from 12 m distance from the MPS and can overcome a 3 m head difference within 40 s.

Although unidirectional pumping was theoretically possible for the “pump/purge to discard” mode, we could not assume plug flow in the cuvettes used. To minimize cross contamination and mixing among consecutive samples, we chose to always reverse pumping direction for all three pumping usage modes, i.e., purge the flow-through cuvettes and storage spiral tubing (described below) with air. Bidirectional pumping was obtained using a custom-made H-Bridge electronic circuit. We built a circuit that inverts polarity at the motor electrodes to trigger either pumping or purging upon a 12 V signal from the controller. The current to power the motor goes directly through the H-bridge and avoids the Arduino, thereby protecting the controller.

Flow-through cuvette

The Spectro::lyser™ probe measures the absorbance of light through the water placed between the emitting and receiving optical lenses. Total absorbance of the sample depends on the optical pathlength and the cumulative absorbance of all light-absorbing elements in water. Although the instrument is designed to be immersed in situ, the application described here keeps the instrument out of the water and uses flow-through cuvettes or cells into which sample water is pumped. Ideally, the optical pathlength should be as long as possible to increase resolution on each measurement and increase the signal to noise ratio, but short enough to prevent too much light from being absorbed to make reliable measurements, which can occur, e.g., in very turbid waters.

To optimize measurements for variable absorbance values and ranges, we used two sizes of cuvettes for the two case studies. In the wetland mesocosm case study, we used a quartz flow-through cuvette (Starna Cells, Inc. model 46-Q-10; Hainault, UK) with an optical pathlength of 10 mm and volume of 4 mL of water. In this configuration, water never touches the instrument optics. In the reservoir case study, the manufacturer’s 40 mL calibration cell for the S::CAN probe was transformed into a flow-through cell by adding inlet and outlet ports to use the default 35 mm pathlength of the Spectro::lyser™ probe for water with low absorbance values.

Sensor quality assurance/quality control (QA/QC)

To minimize sample cross-contamination, the flow-through cuvette volume is pumped through the cuvette several times to ensure thorough rinsing of the manifold pump

cell prior to every measurement being taken. The excess water that passes through the cuvette is temporarily stored in 3 m of tubing spiraled in vertical axis to minimize space (Fig. 1). This step ensures that water present in the cuvette during measurement is fully representative of the water to be analyzed and minimizes cross-contamination from the previous sample by rinsing the cuvette with the sample water (more details below). For the “pump to discard” pumping usage mode, the storage spiral tube is not necessary. It becomes necessary, however, when the sampled water has to be purged back to its source (e.g., in the wetland mesocosm case study below) or purged back to a sampling port for laboratory comparison (e.g., in the reservoir case study below). All tubing in the MPS system is set in an upward vertical position to facilitate drainage and to minimize the volume of residual water in tubing during purging.

The two applications we describe here involved use of the coupled MPS-water quality probe system over several days. To limit biological and chemical fouling of the tubing during deployment, the cuvettes and the instrument optics were cleaned using 2% hydrochloric acid (HCl) solution and mechanically scrubbed using a bristle-brush brush provided by the water quality probe manufacturer every 24–72 h until the absorbance spectrum in air was back to its calibration value. Our experience has shown that significant and rapid fouling on the lenses or the cuvette walls can occur due to Fe and Mn precipitation when reduced waters are oxidized in the cuvette (Etheridge et al. 2013). The magnitude and time for detectable fouling is expected to vary from site to site based on the redox potential of the water, the amount of particulates, and other water characteristics. Consequently, the interval between scrubblings reported here minimized fouling in our case studies, though longer intervals between scrubblings would have likely also sufficed.

MPS micro-controller

An Arduino Mega 53-pin controller chip directs the timings for pumping, purging, and valve actuations. Arduino is a highly customizable open-source electronic system that is supported by a large user community and has many software libraries readily available. The number and sequence of sampling ports can be changed in the program read by the controller. Depending on the distance of tubing to each water source, the timings for pumping and purging can be adjusted on a port per port basis to minimize energy consumption. In the “purge back to source” configuration, the same valve is actuated so that pumping and purging occur through the same port and tubing. For the “purge back to sampling port” and the “purge back to discard” configurations, different valves are actuated for pumping and purging.

The program contains two “sampling sequence” and “sampling cycle” loops. Each “sampling sequence” cycle starts with a 12 V signal sent by the S::CAN probe, normally used to trigger an anti-fouling system at an adjustable time

t_m prior to a measurement. The valve corresponding to the designated port for that point source is actuated. Pumping times and t_m are adjusted together to accommodate sampling sources at variable distances from the probe to ensure that (1) sufficient pumping and rinsing occurs prior to measurement collection, (2) a representative sample with adequate volume is present in the flow-through cuvette, and (3) pumping stops for several seconds when an absorbance measurement is taken. A “sampling sequence” ends after purging. After all designated ports have been sampled, the program resets the numbering to the initial port to start another “sampling cycle.” We have found it useful to have one of the ports dedicated to a control, standard solution, or to pump air to be able to easily distinguish the “sampling sequence” in the absorbance data time series from the probe “sampling cycles.”

Coupled MPS-water quality probe performance testing

Cuvette contamination

In laboratory continuous flow chemical analysis systems (e.g., Segmented Flow Analysis or Flow Injection Analysis), cross-contamination inside the measurement flow-through cell between consecutive samples is minimized by thoroughly rinsing the manifold with the carrier fluid using continuous flow. In our system, however, water droplets left in the tubing from previous pumping create the possibility of cross contamination. This can be alleviated if the manifold and cuvette are continuously rinsed until there is no detectable trace of any previous sample. To quantify the required minimum amount of rinsing of the coupled MPS-water quality probe system, we conducted a “cuvette contamination” experiment. To test the “worst case” scenario of cuvette-contamination, we used the manufacturer’s 40 mL flow-through cuvette because of the higher likelihood of leftover droplets in the system using the larger cuvette than for the 4 mL cuvette. To magnify cross contamination, we alternated pumping water from two point sources in this experiment, one low concentration solution (tap water) and one high concentration solution (tap water spiked at ~ 8.0 mg $\text{NO}_3\text{-N/L}$). We alternated pumping from the two solutions 20 times (10 low concentration measurements and 10 high concentration measurements). We repeated this experiment five times, using a different cuvette rinsing volume each time: 1 \times , 2 \times , 3 \times , 4 \times , and 5 \times times the volume of the cuvette, or 40 mL, 80 mL, 120 mL, 160 mL, and 200 mL pumped past the cuvette. Our expectation was that higher rinsing volumes would result in lower cuvette-contamination.

For each of the five rinsing volumes tested, we evaluated the degree of contamination from the difference between concentrations obtained during alternating low/high solutions and “reference” concentrations for which there was no cross-contamination. To obtain these reference measurements, we repeatedly measured the same high or low solution on alternating ports until the measurements were stable. The reference low concentration was measured at

Table 1. Nitrate-nitrogen (nitrate-N) concentration values for the reference solutions, p -values quantifying the significance of the differences between the treatment and the reference concentrations (Welch t -test on population means) for both high and low concentration solutions, and 95% confidence intervals (95% CI) of the absolute and relative (expressed in %) difference between the treatment and the reference concentrations for both high and low nitrate-N concentration solutions. Asterisks denote non-significance.

Volume of water used to rinse the cuvette	Reference nitrate-N concentrations		p -values		95% CI	
	High	Low	High	Low	High	Low
1X cuvette vol.	8.02 ± 0.02	0.18 ± 0.02	<0.0001	<0.0002	(-0.26, -0.22) (-3.0%; -2.7%)	(0.22, 0.29) (122%, 161%)
2X cuvette vol.	8.02 ± 0.02	0.18 ± 0.02	<0.0001	<0.0001	(-0.09, -0.07) (-1.1%; -0.9%)	(0.04, 0.10) (22%, 55%)
3X cuvette vol.	8.02 ± 0.02	0.08 ± 0.02	<0.0001	<0.0001	(-0.09, -0.07) (-1.1%; -0.9%)	(0.05, 0.07) (62%, 88%)
4X cuvette vol.	8.02 ± 0.02	0.08 ± 0.02	<0.0001	<0.0001	(-0.08, -0.06) (-1.0%; -0.7%)	(0.02, 0.03) (25%, 38%)
5X cuvette vol.	7.92 ± 0.01	0.08 ± 0.02	0.004	0.06*	(-0.02, -0.00) (-0.2%; -0%)	(-0.00, 0.01) (0%, 13%)

*Indicates non-significance.

0.08 ± 0.02 NO₃-N mg/L, while the reference high concentration was measured at 8.02 ± 0.02 mg NO₃-N/L, for an N concentration ratio between the high and low solutions that ranged between 44 and 100 (Table 1). We quantified the differences and the statistical significance between the treatment and reference concentrations using a Welch t -test from populations of 10 treatment and 10 reference values using R software (R Core Development Team 2015).

Cross-contamination

For some applications (see below), it may be desirable to pump and purge water from and to the same point source. In these cases, some of the droplets from the previous sample may contaminate the current source during purging. To quantify the magnitude of this type of contamination, we conducted three experiments with three distinct initially high concentration values (4.65, 6.97, and 8.13 mg NO₃-N/L; Fig. 2). In each experiment, low and high concentration solutions of 500 mL in volume (prepared as described above) were alternately pumped to the water quality probe, the cuvette was rinsed by 1× its volume as described above, and the water was purged back to its point sources so that we could measure the concentration drifts over 30 measurements of each solution ($n = 60$ measurements total). Our expectation was that the measurements of water pumped from the low and high concentrations would increase and decrease, respectively, over time due to cross-contamination with the previous high and low solution samples. From each of the six concentration drifts (i.e., the linear drift over 30 observations measured for both high and low concentrations in the three experiments; Fig. 2; Table 2), we calculated the residual volume, V_{res} , that could

potentially contaminate point sources during each purging using the following equation:

$$V_{\text{res}} = \left(\frac{C_{\text{final}} - C_{\text{initial}}}{C_{\text{alt}} - C_{\text{initial}}} \right) \cdot \frac{V}{(p/2)} \quad (1)$$

Where C_{final} and C_{initial} are the final and initial nitrate concentrations measured from each concentration drift, C_{alt} is the concentration of the alternate solution (i.e., for an upward drift, C_{alt} is the high concentration, and for a downward drift, C_{alt} is the low concentration), V is the volume of the point source solution, which stayed stable at 500 mL and $(p/2)$ is the number of measurements per point source (e.g., $60/2 = 30$). C_{alt} was treated as constant and equal to the average over the 30 purges of the alternate concentration. We used the global calibration from the S::CAN instrument to calculate the concentration of nitrate in each measurement.

Concentration computations using the S::CAN probe

Chemometrics algorithms

As noted above, the S::CAN probe measures light absorbance on wavelengths ranging from 200 nm to 737.5 nm on a 2.5 nm resolution. The probe is fitted with algorithms that interpret the absorbance spectrum to calculate analyte concentrations; however, the manufacturer recommends that the calculated concentrations be locally calibrated with laboratory analyses. For nitrate concentrations within validated ranges, such calibration may correspond to an offset or slope change specific to the matrix of water being analyzed (S::CAN Spectrometer Probe Manual 2011).

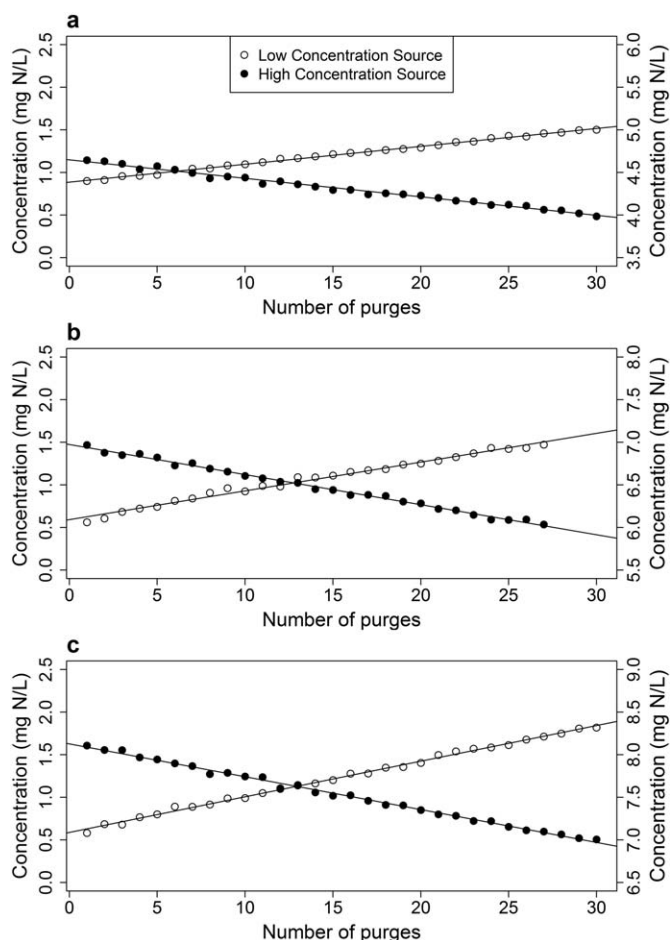


Fig. 2. Increasing dilution and concentration over time of the original high and low nitrate-N concentration solutions, respectively, due to cross contamination when pumping from and purging to the same point source. Black circles represent measurements of the high nitrate-N concentration solution and white circles represent measurements of the low nitrate-N concentration solution after each consecutive purge of the coupled MPS-water quality probe system. Each of the panels show the experiment repeated for a high N solution initially measured at (a) 4.65 mg $\text{NO}_3\text{-N/L}$; (b) 6.97 mg $\text{NO}_3\text{-N/L}$ and (c) 8.13 mg $\text{NO}_3\text{-N/L}$; the low N solution for all three experiments was initially measured at 0.59 mg $\text{NO}_3\text{-N/L}$. Note that the y-axes differ among panels.

To examine the concentrations of analytes other than those with established global S:CAN calibrations (i.e., nitrate, DOC, TOC, and turbidity), we used the Partial Least Square Regression (PLSR) package (Mevik et al. 2011) in the R statistical framework (R Core Development Team 2015) to correlate absorbance data with phosphate, iron, and silica, following the procedure detailed in Etheridge et al. (2014). Briefly, PLSR is a chemometric technique which reduces the large number of absorbance measurements from each wavelength in principal component vectors to best explain measurement variance. This statistical technique is well suited for situations in which the explanatory variables are highly autocorrelated, as is expected by absorbance values from

sequential wavelengths. The optimum number of PLSR components for each analyte was chosen as the lowest number of components for which the root mean square error of concentration prediction (RMSEP) was at or near its minimum value.

Results

Performance testing

Cuvette contamination

Our data indicate that cuvette contamination between the alternating low and high solutions is detectable and significant after rinsing the cuvette with 1 \times , 2 \times , 3 \times , and 4 \times times the cuvette volume for the 40 mL cuvette (as determined by significant differences between the mean concentrations; Table 1). However, after rinsing the cuvette with five times its volume, no significant differences between the reference and low concentration solution were observed (Table 1). While 5 \times rinsing would be ideal, it requires much longer pumping times and consequently fewer measurements over time. In our test, the sampling cycle time for 5 \times rinsing was 270 s, while that of 3 \times rinsing only lasted 205 s, i.e., 24% less time. While there was still statistically significant cuvette contamination detected for all but 5X rinsing, in practical terms it may be just as meaningful to evaluate the absolute difference between the reference and the measured concentrations. For 2 \times rinsing, our results show that high concentrations were underestimated by about 1% (Table 1). For many applications, this may equate to acceptable concentration differences or be at the limit of detection. However, should the precision expectations be very high, particularly for low concentrations, then 5 \times rinsing may be required. For practical purposes, given that the concentration ratio between consecutive samples is less than 20 in the vast majority of cases, rinsing the cuvette with 3 \times its volume should be sufficient for avoiding cuvette contamination.

Cross-contamination

Additional care is also needed when the “purge to source” configuration is used. In this configuration, the 500 mL point sources became contaminated over time as expected, i.e., diluted or concentrated by the alternate low or high samples, respectively. The dilution of the high nitrate solution and the concentration of the low solution increased as a function of the concentration difference between the two solutions: the cross contamination was greatest using a high nitrate solution initially measured at 8.13 mg $\text{NO}_3\text{-N/L}$, in comparison to high N solutions initially measured at 4.65 or 6.97 mg $\text{NO}_3\text{-N/L}$ (Fig. 2).

From the concentration drifts measured, the estimates of the potentially contaminating residual volume in each experiment varied from 2.6 mL to 2.9 mL (Table 2). Thus, when pumping and purging water from and to the same point source using the manufacturer’s 40 mL flow-through

Table 2. Estimates of the apparent contaminating residual volume V_{res} in mL remaining in the cuvette after a sample that could potentially contaminate the consecutive source using the manufacturer's 40 mL flow-through cuvette when using the "purge back to point source" configuration.

High concentration source			Low concentration source		
Initial nitrate-N concentration (mg NO ₃ -N/L)	V_{res} (mL)	95% Confidence intervals	Initial nitrate-N concentration (mg NO ₃ -N/L)	V_{res} (mL)	95% Confidence intervals
4.65	2.89	(2.83, 2.95)	0.89	2.79	(2.76, 2.83)
6.97	2.77	(2.72, 2.81)	0.59	2.64	(2.58, 2.70)
8.13	2.56	(2.53, 2.59)	0.59	2.77	(2.74, 2.80)

cell, potentially up to 3 mL of the previous sample can contaminate the point source. This suggests that the "purge to source" configuration should only be used with confidence in the cases for which the effects of contaminating residual volume remain undetectable, i.e., the dilution or concentration would remain small enough to be within the instrument measurement uncertainty, which in our case here was estimated to be 0.02 mg NO₃-N/L of nitrate as the 95% confidence interval from 20 repeated measurements. These conditions can be met when the point source volume is large compared to the contaminating residual volume and when the difference in concentrations between consecutive samples is relatively small. For example, assuming 3 mL of potentially contaminating volume for two alternating point sources of 20 L each with concentrations that differ by 2 mg NO₃-N/L, it would take more than 60 consecutive purges to the point source to detect the effect of cross-contamination. The number of purges would increase if the effective contaminating volume decreased (e.g., by using a smaller volume flow-through cuvette, such as a smaller volume quartz flow-through cuvette) or if there was a smaller difference in concentrations between consecutive measurements. In all cases, these results suggest that the "purge back to source" configuration should only be used within the limits defined here.

Two case studies

Application 1: Using the coupled MPS-water quality probe system to quantify the effects of water current velocity on constructed wetland treatment efficiency

Hyporheic advective exchange in wetlands

Nitrate removal processes (e.g., denitrification) in wetlands that receive excess nitrate are limited, in part, by the ability of nitrate to move from the water column to sediment denitrifying microsites (reviewed by Birgand et al. 2007). In stagnant water, this transport is diffusive in nature and therefore slow. Many studies conducted in streams have shown that nitrate exchange between the water column and underlying substrate (the hyporheic zone), can be greatly enhanced by advective transport of water into the sediment. This advective transport can occur as a result of increased

water current velocity above the sediment's uneven surface or obstacles above the sediment, such as sand deposits in streams (e.g., Savant et al. 1987; Thibodeaux and Boyle 1987; Huettel et al. 1996; Elliott and Brooks 1997; Hutchinson and Webster 1998), or a loose matrix of debris from dead macrophyte stems deposited onto wetland sediments.

We hypothesized that increasing the current velocity of water above the sediment bottom in constructed treatment wetlands would induce advective exchange between the water column and the sediment, thereby increasing denitrification and enhancing treatment efficiency. The implication is that it may be possible to construct wetlands to be more efficient in removing nitrogen per unit area by increasing water current velocity over the sediments.

To test this first hypothesis, we conducted a mesocosm experiment in which we recirculated water overlying undisturbed large sediment cores collected from a wetland at different velocities. We evaluated nitrogen removal (treatment efficiency) from the kinetics of the decreasing nitrate concentration over time in the overlying water. Our second hypothesis was that the use of the coupled MPS-water quality probe system would both improve our measurement of nitrogen removal kinetics and provide information on the spatial variability of nitrogen removal in replicated wetland mesocosms.

Experimental set-up and mesocosm description

To create the mesocosms, we collected three undisturbed whole core wetland samples (56 cm in diameter, 15 cm deep) by inserting large 30 cm-long PVC rings of the same diameter into the organic substrate of a riparian wetland adjacent to eutrophic Rocky Branch stream which receives pulses of high nitrate concentrations (~2–5 mg NO₃-N/L) and runs through the North Carolina State University campus (Raleigh, North Carolina, U.S.A.; 35°46'50" N, 78°40'8" W). To ease insertion of the rings and reduce disturbance of the cores, a machete blade was used to cut vertically into the substrate. After the rings were inserted, a 60-cm wide aluminum blade was used to cut horizontally and provide support under the cores, which were then excavated and transferred over 70 cm diameter Plexiglas disks as core

bottoms, brought back to the lab, and sealed at the bottom by pressing the rings against a neoprene seal using turnbuckles.

We report three experiments that corresponded to three different water recirculation velocities (0, 3, and 11 cm/s). Each experiment consisted of three replicated sediment mesocosms and one control mesocosm that did not have any sediment on its Plexiglas bottom. Ten cm of Rocky Branch stream water was added to all four mesocosms, which was recirculated individually in each mesocosm at a stable velocity throughout the experiment (16.6 L of total water per mesocosm). To compensate for water losses from evaporation, deionized water was automatically added through a Mariotte jar system which effectively maintained the water column height constant. Water velocities were controlled using submerged aquarium pumps, installed parallel to the tangent of the PVC ring. The intake and outlet valves on the pumps were opened and closed to create higher or lower velocities, respectively, in the three different experiments.

The mesocosms were large enough to create the conditions for circular racetrack flumes and 10 cm deep. Flow patterns in racetrack flumes are complicated and involve advective cells and dead zones at their centers (e.g., Khalili et al. 1997, 1999; Basu and Khalili 1999). To limit dead zones, flow in the mesocosm centers was excluded by adding and centering 20-cm diameter stainless steel cylinders, leaving flow to occur in a circular shape. Velocity values used for analysis were measured at the center of the cross-section of the doughnut channel using a Marsh-McBirney Flo-Mate™ (Frederick, Maryland, U.S.A.).

Experimental data collection

We quantified nitrate removal efficiency by measuring the rate of decreasing nitrate concentrations in the mesocosms. We first spiked the water overlaying the sediment with potassium nitrate to reach 2–3 times the background nitrate concentrations, which varied between 1.5 and 3.0 mg NO₃-N/L. To reduce nitrate assimilation or release due to photosynthetically-active vegetation and algae, macrophyte vegetation in the mesocosms was clipped and all incubations were conducted in the dark. All cores were incubated at the same near constant temperature (20°C ± 1°C) in a controlled temperature room over 30 h, the length of each of the three experiments.

During the water recirculation, the coupled MPS-water quality probe system was used to measure nitrate concentrations on a sampling sequence of every 2.5 min, resulting in a 10-min sampling cycle or 10-min resolution data for each of the three treatment mesocosms and the control. The water intake tubing was placed in the mesocosms' channel center, 5 cm above the sediment, with one point source per mesocosm. The system was configured to pump from and purge water back to the same mesocosm. Using the 4 mL quartz cuvette, the contaminating residual volume was

estimated to be no more than 1 mL, and the concentration difference between consecutive samples was always less than 2 mg NO₃-N/L, so that cross-contamination could not be detected 30 h after the beginning of the experiment.

Nitrate concentrations given by the Spectro::lyser™ were compared to and corrected by an offset to match laboratory values for each experiment (details in Horstman 2012). We removed 8 mL of water from each mesocosm at ~12 h frequency for manual nitrate measurements; these samples were immediately passed through 0.2 μm filters and kept at 4°C until analysis on a Lachat Quik-Chem 8000 (Lachat Instruments, Loveland, Colorado, U.S.A.) following the Quik-Chem Method 10-115-10-1-B. Between each of the three different recirculation experiments, all of the overlying water was siphoned out from each mesocosm, which were left water-saturated until the next experiment. New stream water was then added to re-fill the mesocosms, recirculated at the desired velocity, and spiked with nitrate following the same procedure.

Nitrate removal rates kinetics

We used the nitrate concentrations measured by the coupled MPS-water quality probe system to estimate nitrate removal rates. To quantify nitrate uptake or removal rates (R), i.e., the mass of nitrate removed per projected surface area per time (e.g., mg NO₃-N/m²/d), in stream and wetlands, four general kinetics models have been proposed: zero order rate models (e.g., Horne 1995; Mitsch et al. 2005) where the rates are independent of the water column nitrate concentration (i.e., $R = k$, where k is a constant); first order models (e.g., Stream Solute Workshop 1990; reviewed in Birgand et al. 2007), where the rates are proportional to the water column nitrate concentrations (i.e., $R = \rho C$, where ρ is the proportionality coefficient otherwise referred to as the mass transfer coefficient or uptake velocity, and C is the water column nitrate concentration); efficiency loss models (O'Brien et al. 2007), where the rates are less than proportional to the water column nitrate concentrations (i.e., $R = \gamma C^\alpha$, where α is less than 1 and higher than 0, and γ is the mass transfer coefficient); and Michaelis-Menten models (i.e., $R = \frac{R_{\max} \cdot C_0}{K_s + C_0}$, where R_{\max} is the maximum nitrate removal rate, C_0 is the initial nitrate concentration, and K_s is the half saturation constant; e.g., Bernot and Dodds 2005).

For the simplicity of its application, and possibly also due to the lack of data, the first order model is the one most often used in streams (e.g., Smith et al. 1997; Alexander et al. 2000) and wetlands (e.g., Kadlec and Wallace 2009). Here, we used the high-resolution nitrate data collected by the coupled MPS-water quality probe system to compare the performances of the first order model to those of the efficiency loss and the Michaelis-Menten models (Fig. 4; Table 4) by fitting the models to the measured nitrate concentrations and removal rates using the nonlinear least square method package *nls* in the R software.

Table 3. Summary statistics of the model goodness of fit (auto-correlation function (ACF): Yes, when residuals show significant auto-correlation, No, otherwise) and model parameter values (\pm standard error from the nonlinear regression parameter estimate) for the first order, efficiency loss (Eff Loss), and Michaelis-Menten models; estimated time it would take to lower nitrate concentrations from 5 mg to 0.25 mg nitrate-nitrogen ($\text{NO}_3\text{-N}$)/L using the first order and efficiency loss models; and the percentage difference between the estimated times from the Eff loss and first order models.

		0 cm/s			3 cm/s		11 cm/s		
		Rep1	Rep2	Rep3	Rep1	Rep3	Rep1	Rep2	Rep3
First order model	ACF	Yes	Yes	Yes	Yes	Yes	Yes	Yes	Yes
	ρ (m/d)	0.15 ± 0.00	0.19 ± 0.00	0.14 ± 0.00	0.27 ± 0.01	0.22 ± 0.002	0.28 ± 0.002	1.02 ± 0.02	1.25 ± 0.02
Efficiency loss model	ACF	No	No	No	No	No	No	No	No
	γ (m/d)	0.26 ± 0.01	0.29 ± 0.01	0.35 ± 0.02	0.21 ± 0.01	0.35 ± 0.01	0.37 ± 0.001	1.23 ± 0.04	1.54 ± 0.03
Michaelis-Menten model	A	0.38 ± 0.07	0.52 ± 0.04	0.22 ± 0.04	0.63 ± 0.02	0.59 ± 0.02	0.75 ± 0.02	0.77 ± 0.04	0.81 ± 0.01
	ACF	Yes	No	No	No	Yes	No	No	No
	K_s (mg $\text{NO}_3\text{-N/L}$)	2.28 ± 0.74	2.04 ± 0.41	0.87 ± 0.23	0.64 ± 0.05	4.30 ± 0.49	8.79 ± 0.68	3.98 ± 0.29	11.1 ± 0.75
	R_{\max} (mg $\text{N/m}^2/\text{d}$)	733 ± 116	856 ± 82	578 ± 36	972 ± 15	1650 ± 112	3397 ± 191	6142 ± 304	17106 ± 945
Time to lower [$\text{NO}_3\text{-N}$] from 5.0 to 0.25 mg $\text{NO}_3\text{-N/L}$ (days)	First order	2.00	1.54	2.06	0.94	1.34	1.06	0.29	0.28
	Eff loss	1.43	1.18	1.17	0.65	0.96	0.84	0.25	0.19
Percentage difference in time estimate		40%	30%	77%	45%	39%	25%	16%	42%

Mesocosm experimental results

We observed that nitrate removal is variable but increases with current velocity. Nitrate concentration decreases measured for 0, 3, and 11 cm/s water current velocities for the three mesocosm replicates (rep1, rep2, and rep3) and the control by the coupled MPS-water quality probe system are illustrated in Fig. 3 (data for rep2 at 3 cm/s were discarded because the water intake became clogged during the experiment). Nitrate concentrations for the control remained constant over time, indicating no detectable removal. Nitrate removal, indicated by the slope of the concentration time series in Fig. 3, increased with increasing velocity, supporting our initial hypothesis.

However, while nitrate removal rates for rep2 and rep3 had similar responses to increased velocity, the response of rep1 at 11 cm/s yielded much lower rates. After careful visual inspection, the rep1 sediment surface appeared “smooth” compared to the other two treatment mesocosm sediment surfaces, suggesting that the sediment pores and irregularities clearly visible at the sediment surface for rep2 and rep3 may have been clogged by particles resuspended by water current during the experiments. The smooth surface in rep1 may have dramatically decreased the advective exchange that is induced by velocity over porous sediment irregularities (e.g., Hutchinson and Webster 1998; Marion et al. 2002;

Packman and Salehin 2003; Salehin et al. 2003; Packman et al. 2004), hence reducing the ability for nitrate to reach denitrification microsites. Our experiment thus suggests that moving water above uneven, porous, and organic constructed wetland sediments may increase the ability of water column nitrate to penetrate into the reactive sediment, where it may be removed.

Our results show that the first order rate kinetic model appears inappropriate. It does not fit the observed data well (Fig. 4), as the model residuals are not randomly distributed. This is confirmed by the autocorrelation function (ACF), which shows that the residuals are significantly auto-correlated. In contrast, the efficiency loss model provides the best fit to the data as the model residuals are randomly distributed and not significantly auto-correlated for all experiments and replicates. The Michaelis-Menten model also generally performs well, although there are two cases in which the model residuals are not randomly distributed and are significantly auto-correlated (Fig. 4; Table 3). Similar to our observations, O’Brien et al. (2007) have shown that the efficiency loss model fitted stream nitrate removal better than the first order or the Michaelis-Menten models. Furthermore, the nitrate concentration time series in Fig. 3 did not exhibit any linear patterns, which ruled out the use of zero order models.

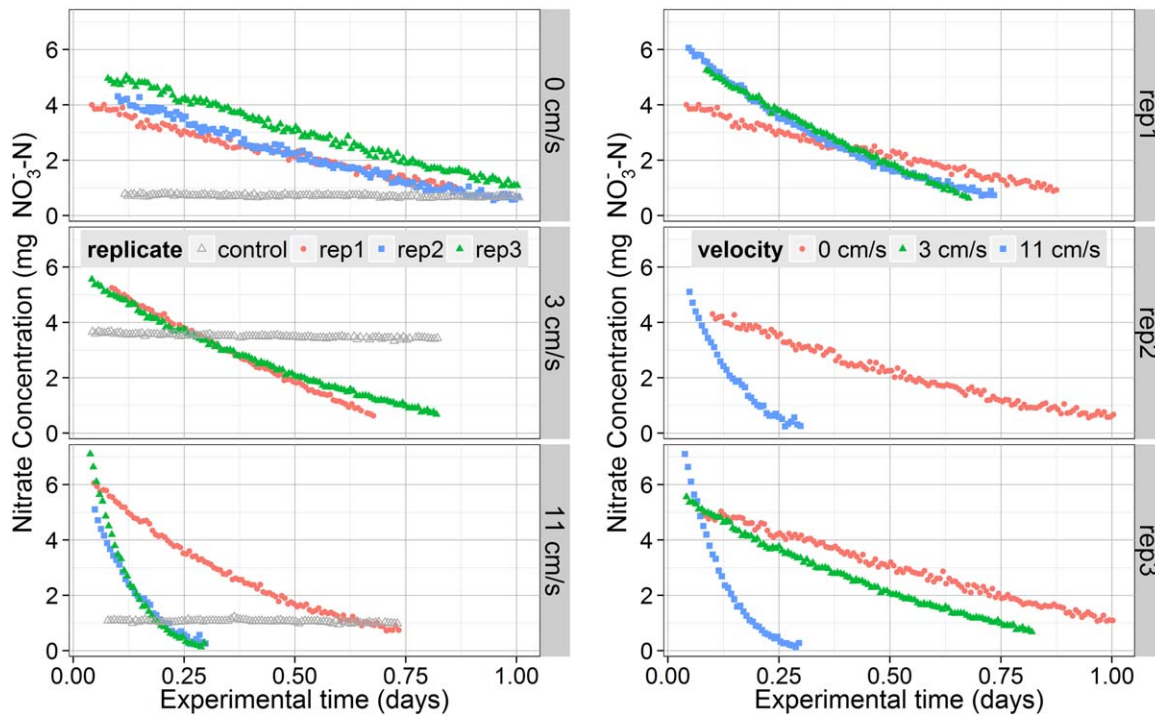


Fig. 3. The decrease in nitrate-N concentrations over time for three mesocosm experiments with different recirculation velocities (0, 3, and 11 cm/s). Each experiment consisted of three large constructed wetland sediment core replicates (denoted as rep1, rep2, and rep3) and one control with no sediment; in the left panel, data are organized as a function of the velocity treatments and in the right panel, as a function of the replicates. Data for rep2 of the 3 cm/s experiment were omitted because the water intake became clogged during the experiment.

Without the coupled MPS-water quality probe system, nitrate concentrations would have been obtained from manual samples of the water in the laboratory, which would have substantially reduced the temporal resolution of sampling points for logistical reasons. Using traditional sampling methods (e.g., by collecting water from the mesocosms ~ 5 times over 24 h for nitrate analysis in the laboratory), it would have been impossible to show that the first order model was inappropriate, or to show that the efficiency loss model was significantly better in calculating nitrate removal.

Using both the first order and efficiency loss models (the worst-fitting and best-fitting models tested, respectively), we calculated the estimated time it would take to decrease nitrate concentration from 5 to 0.25 mg $\text{NO}_3\text{-N/L}$ (typical values representing high and low nitrate concentrations observed in constructed wetlands; Kadlec and Wallace 2009), for each replicate and each experiment (Table 3). Our results show that the first order model, which is the most widely used, tends to overestimate the time it would take to remove nitrate by $\sim 30\text{--}40\%$, compared to the efficiency loss model, which fits the data much better. These results suggest that the common approach to predicting wetland nitrate removal using the first order model may be too conservative and may significantly under-predict removal efficiency.

Moreover, our data also suggest that increasing water movement in wetlands greatly increases nitrate removal

efficiency from its default stagnant state (Table 3). Using the efficiency loss model results in Table 4, our data indicate that nitrate removal processes may be occurring four to six times more quickly when the water velocity is increased from 0 to 11 cm/s. Initial removal rates reached up to ~ 6 g/ $\text{m}^2\text{/d}$, which correspond to the upper range of rates reported in treatment wetlands (Kadlec and Wallace 2009). Interestingly, the exponent in the efficiency loss model also increased with increasing velocity, and so do the R_{max} values. Increasing water velocity could therefore decrease the duration of time needed for nitrate removal processes in constructed wetlands. In summary, the use of the coupled MPS-water quality probe system in this application has shown, potentially for the first time, that the common first order rate kinetic approach is too conservative for estimating nitrate removal and that recirculating water in wetlands is crucial for stimulating nitrate removal processes.

Application 2: Whole-ecosystem responses to hypolimnetic oxygenation in a reservoir

Managers and utilities are increasingly using oxygenation systems to improve water quality in lakes and reservoirs used for drinking water (Singleton and Little 2006; Gerling et al. 2014, 2016). While oxygenation has been shown to successfully decrease soluble nutrient and metal concentrations over day to week time scales, the effects of oxygenation on shorter (minute) time scales remain unknown, especially at

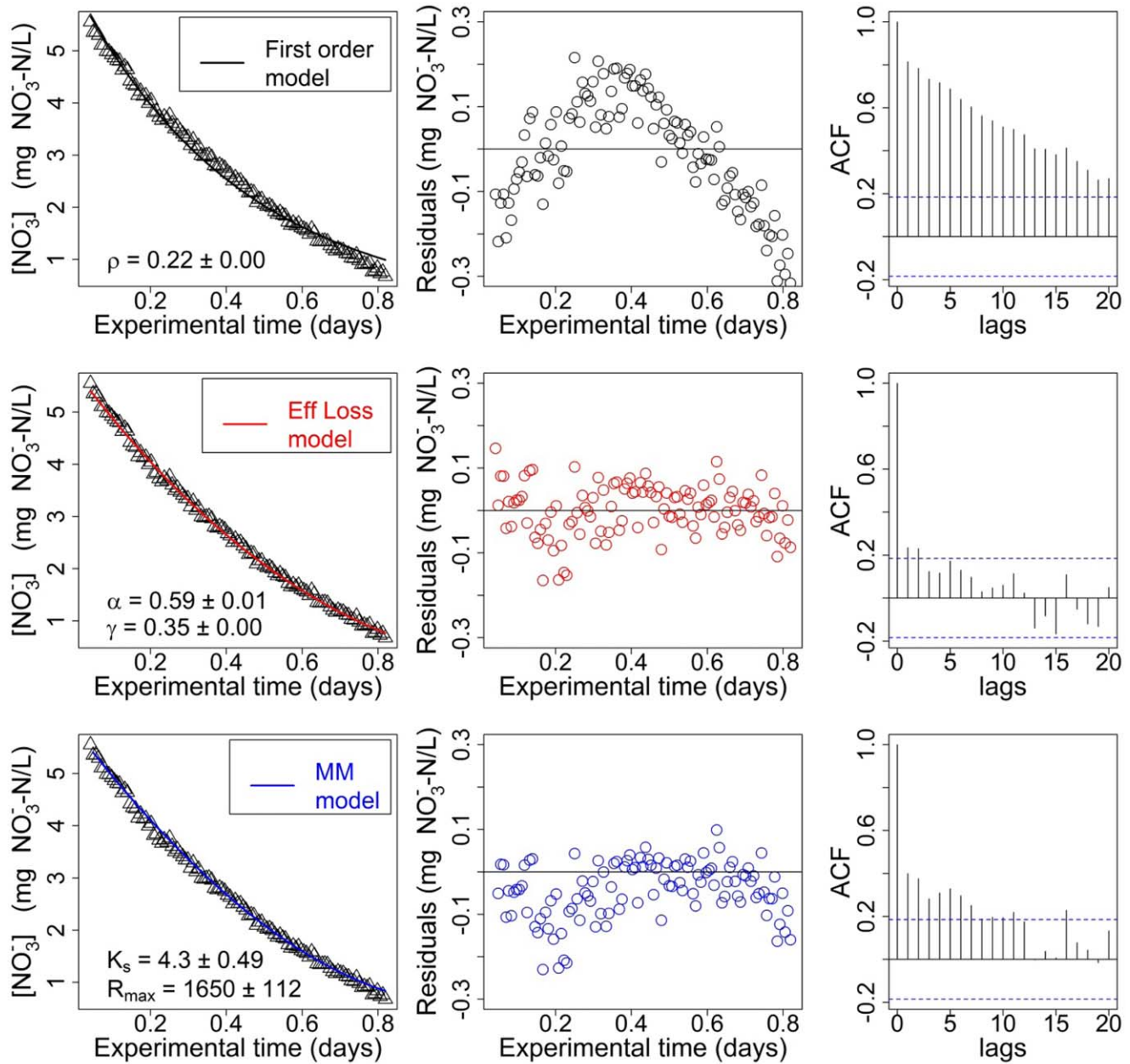


Fig. 4. Application of first order, efficiency loss (Eff Loss) and Michaelis-Menten (MM) models (black, red, and blue solid lines, respectively) to nitrate concentration decreases (triangles) measured by the coupled MPS-water quality probe system on mesocosm replicate 3 for 10 cm of overlying water recirculated at 3 cm/s. Residuals of the efficiency loss model (red circles) are randomly distributed, as most of the lag values are within the significance interval (horizontal blue dotted lines) on the autocorrelation function (ACF) plot; residuals of the first order and Michaelis-Menten models are not randomly distributed (black and blue circles) and most lags are above the significance level of autocorrelation.

the whole-ecosystem level. We deployed the MPS-water quality probe system to measure whether the transition of an anoxic hypolimnion to oxic conditions would be accompanied with rapid changes in nutrient and metal concentrations with the altered redox potential.

We examined the effects of experimentally-manipulated redox conditions on nutrient and metal concentrations in Falling Creek Reservoir (FCR), a eutrophic drinking-water reservoir

owned and operated by the Western Virginia Water Authority (Gerling et al. 2014, 2016). FCR is located in Vinton, Virginia, U.S.A. (37°18'12" N, 79°50'14" W) and is a small reservoir ($Z_{\text{max}} = 9.3$ m, surface area = 0.12 km², and maximum volume = 3.1×10^5 m³), with one inflowing stream (Gerling et al. in press). The reservoir is typically thermally stratified from May to October. Throughout this experimental monitoring period, the water residence time in the reservoir was ~38 d.

Table 4. Summary statistics for the Partial Least Square (PLS) calibration regressions used to estimate nitrate, phosphate, dissolved iron, and dissolved silica concentration at nine depths at the Falling Creek Reservoir in July 2014.

Parameters	Number of samples used for calibration	Concentration range ($\mu\text{g/L}$)	Number of components used in PLSR	R^2	2X Residual Standard error ($\mu\text{g/L}$)
$\text{NO}_3\text{-N}$	35	1–5	7	0.89	0.86
$\text{PO}_4\text{-P}$	36	3.5–10	7	0.89	1.08
Dissolved Fe	27	100–1000	5	0.94	146
Dissolved Si	26	5000–7500	6	0.83	300

In 2012, a side-stream supersaturation (SSS) oxygenation system was deployed in FCR to increase hypolimnetic oxygen concentrations. The SSS pumps hypolimnetic water from 8.5 m depth onshore to an oxygen contact chamber, injects concentrated oxygen gas under high pressure, and then returns the super-saturated oxygenated water at the same temperature and depth to the hypolimnion (see Gerling et al. 2014 for more details on the engineering design of the system). The oxygenated water is ejected from the SSS via eductor nozzles into the hypolimnion under pressure, resulting in a uniformly-mixed hypolimnion with similar oxygen concentrations above and below the SSS distribution header. Initial operation of the SSS demonstrates that the system is able to successfully increase oxygen concentrations in the water column while maintaining thermal stratification (Gerling et al. 2014). Once activated, the SSS increases oxygen concentrations in the bulk hypolimnion through mixing via eductor nozzles within an hour.

We intensively monitored FCR with the MPS-water quality probe system described in this article for 9 d in summer 2014. The system was deployed on a permanent platform built 1.5 m above the water's surface at the deepest site of the reservoir. Ten ports of the multiplexer were used pumping water from nine depths (0.1, 0.8, 1.6, 2.8, 3.8, 5, 6.2, 8.0, and 9.0 m, corresponding to the intake depths for the water treatment plant), while the tenth port was used to pump air for reference purposes. Water was not purged back to its source, but was purged to the tenth port, from which series of manual samples were taken for laboratory analyses. Pump timings were adjusted to account for water in the tubing from the previous cycle to be pumped out, and for "new" water to be pumped in the cuvette for at least the equivalent of 3X cuvette volumes for rinsing and such that the tubing coil past the cuvette be filled with new water for manual sampling purposes. As a result, in addition to cuvette rinsing, the immersed tubing was thus rinsed by 2.5 to 10X the tubing's volume of new water, depending on the tubing length. The sampling sequence for each port lasted 3 min, for a final sampling cycle time resolution of 30 min at each of the nine depths.

As the total absorbance was expected to be low, the S::CAN spectrometer was outfitted with the 40 mL manufacturer cuvette modified as a flow-through cell to maintain

35 mm measurement path length. The MPS-water quality probe system continuously cycled from the nine depths throughout the monitoring period, except for 15 min breaks every second or third day to clean the cuvette and the optics with cotton swabs soaked in 2% HCl to prevent metal precipitate from oxidizing on the sensor.

From manual samples described earlier, we measured a suite of chemistry response variables from the sampled reservoir water. Water samples from each of the nine depths were collected for metals and nutrient analyses on 29 June (both 1 h before and 1 h after the SSS was activated), 30 June, and 07 July, providing $n = 36$ calibration data points total. On each sampling day, we filtered water from each depth through GF/F Whatman filters (0.7 μm pore size) into acid-washed bottles, which were frozen until analysis. These samples were analyzed for nitrate-nitrite ($\text{NO}_3\text{-NO}_2$), and phosphate (PO_4^{3-}) on a Lachat following the Quik-Chem Method 10-115-10-1-B. Second, collected water from each depth was used to measure dissolved fractions (filtered through 0.4 μm pore size filters) of Si and Fe using a Thermo Electron X-Series inductively coupled plasma mass spectrometer (ICP-MS) per Standard Method 3125-B (APHA, AWWA, and WEF 1998). ICP-MS samples and calibration samples were prepared in a matrix of 2% nitric acid by volume.

We began the experiment in the evening of 27 June 2014, when the SSS was deactivated and the hypolimnion was anoxic. At 11:00 on 29 June 2014, the SSS was activated to continuously add 25 kg O_2 /day to the hypolimnion. We monitored the increase in hypolimnetic oxygen and its effects on metals and nutrient concentrations in the water column for 7 d at a 30 min resolution, until 06 July 2014. The changes in temperature, dissolved oxygen, and chlorophyll *a*, and turbidity with depth are reported elsewhere (Gerling et al. 2016).

Co-variability between concentrations and "color matrix" of water

We were able to establish highly significant correlations between absorbance spectra and nitrate, phosphate, iron, and silica concentrations in the lake (Table 4). To our knowledge, this is the first report of the use of in situ absorbance to measure metal and silica concentrations in lakes. These results must be taken with caution, however. The number of

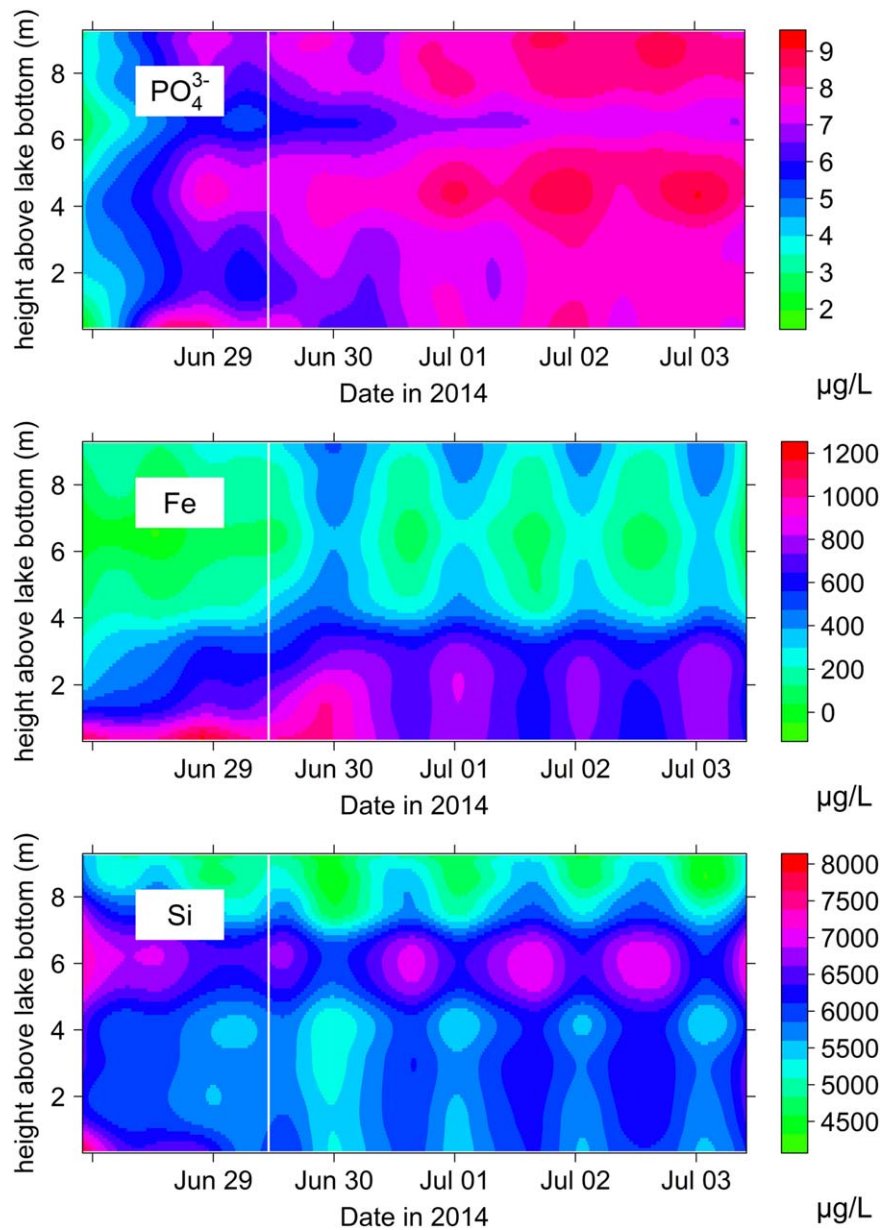


Fig. 5. Concentration variations of dissolved PO_4^{3-} , Fe, and Si in Falling Creek Reservoir as a function of depth and time, obtained from 30-min data for nine depths using the coupled MPS-water quality probe, before and after oxygenation of the hypolimnion (vertical white line).

samples for calibration is relatively small ($n = 36$), and the number of components used to obtain PLSR regressions was higher than 10% of the number of calibrating samples, which has been suggested as a potential guideline for PLSR (Mevik et al. 2011). In addition, the measurement uncertainties in elemental concentrations calculated for the water quality probe (reported in Table 4), are larger than those generally accepted in the laboratory. Despite these uncertainties, however, the general trends we observed in elemental concentrations through the water column in response to oxygenation were robust to the number of components used in the PLSR regressions (data not shown).

We detected large fluctuations in dissolved Fe and Si concentrations that coincided with the shift in redox potential upon the initiation of oxygenation. The thermocline depth located at 4 m (Gerling et al. 2016) provides a sharp contrast to epilimnetic and hypolimnetic conditions. The activation of oxygenation at midday on 29 June 2014 (vertical white lines in Fig. 5) is accompanied with rapid changes in the hypolimnion, particularly at the reservoir sediments, where dissolved Fe and Si concentrations decrease within a few hours of oxygenation. Our data suggest that the reservoir sediments seemed to have been a hot spot for anoxic release of Fe prior to oxygenation. Interestingly, our results suggest

that there may be diel concentration patterns and large concentration changes occurring spatially and in time throughout the water column. The cause of these diel changes is unknown, but may be related to light availability in the hypolimnion, as the oxygen addition rate was constant throughout the oxygenated monitoring period. Diel shifts in dissolved organic matter and other elements have also been measured in other lentic water bodies (e.g., Watras et al. 2015, 2016), which have been attributed to a suite of biogeochemical processes. Throughout the experimental period, the compensation depth was estimated to be ~ 7.6 m from Secchi disk measurements, indicating that light was able to penetrate through most of the hypolimnetic volume, which was substantially mixed during oxygenation.

Although nitrate is known to absorb light in the 220–230 nm range (Suzuki and Kuroda 1987; Crumpton et al. 1992), the concentration level observed in the reservoir (1–5 $\mu\text{g N/L}$; Table 3), is lower than the instrument detection and resolution limits. We thus believe that not only for nitrate but for all four parameters reported here, the highly significant PLSR regressions are evidence of co-variability between the absorbance spectra, or the “color matrix” of the water, and parameter concentrations. Etheridge et al. (2014) proposed the same explanation when monitoring a brackish salt marsh in North Carolina. We highly recommend future testing and validation for using absorbance data as a surrogate to measure a large suite of parameters, as this method holds great promise for measuring a wide range of elements in situ and at high-frequency temporal resolution. The relatively buffered variations of hydrological conditions in reservoirs and lakes, compared to those in streams and rivers, suggest that lentic waterbodies may be good candidates for deriving correlations between the color matrix of water and chemical concentrations. In summary, the use of the coupled MPS-water quality probe system in this application has shown minute-resolution changes in the concentrations of elements that have heretofore never been measured in situ in response to altered redox conditions, as well as large diel shifts in multiple elements occurring in the absence of changes in redox.

Discussion and conclusions

Until very recently, one could obtain high spatial resolution in water quality variables over a short period (e.g., one day) by sampling many locations manually or using sampling instruments to collect samples at multiple depths (e.g., Morsy 2011). Alternatively, researchers could obtain high temporal resolution using automatic samplers or using continuous sensors. Thus, high resolution was achievable either in space *or* in time, but almost never together. The increasing availability of in situ high frequency water quality probes is revolutionizing water quality monitoring, and more importantly, has the potential to substantially advance our

understanding of aquatic biogeochemistry. Our coupled MPS-water quality probe system presented here is able to extend temporal high-frequency capabilities to a greater spatial resolution, permitting up to 12 additional measurements from nearby sites or replicated units. The results of the performance testing have shown that when the coupled MPS-water quality probe system is used within the limits defined in this article, it can provide reliable high-frequency measurements for a variety of different elements. We note that combined resolution in space and in time has also been achieved in lentic ecosystems using commercially available in situ vertical profilers, which automatically sample water quality variables with sensors at multiple depths in a profile (e.g., YSI Environmental 2006a,b). These systems have specifically been designed for water bodies several meters deep, while our system has been designed for these and other uses.

Observing variability at new scales

Continuous high-frequency water quality data at a single point in a watershed enables capturing rare events (“hot moments,” McClain et al. 2003) that have a disproportional impact on nutrient and material fluxes. Our coupled MPS-water quality probe system opens the possibility to detect not just hot moments (temporal variability) but also identify “hot spots” (spatial variability) in the landscape (e.g., McClain et al. 2003; Vidon et al. 2010). Consequently, we can now observe biogeochemical processes that are linked in time and space. The power of the system for detecting high-frequency fluxes at multiple sites or depths was particularly apparent in the reservoir application, when a hot moment occurred in response to a sudden change in the redox conditions in the hypolimnion. After the initiation of oxygenation, high dissolved Fe concentrations at the anoxic sediments decreased by a factor of two, likely due to precipitation in increasingly oxic conditions. The slight peak of Fe at the sediments a few hours after oxygenation began is likely due to the SSS’s mixing of the hypolimnion, entraining water with high dissolved Fe concentrations from the sediments to higher depths in the water column, prior to an overall decrease in concentrations.

Furthermore, the MPS-water quality probe system also revealed diel fluctuations of nutrient and metal concentrations synchronized in the epilimnion and hypolimnion, which has been observed in other aquatic systems (e.g., Pellerin et al. 2009, 2012; Nimick et al. 2011; Cohen et al. 2012, 2013; Snyder and Bowden, 2014; Watras et al. 2015). Silica concentrations peak during early afternoons at the thermocline, while Fe concentrations are at their lowest at the same time in the epilimnion, which may be due to autotrophic and heterotrophic immobilization. By comparison, while dissolved Fe and Si concentrations appear to vary almost by a factor of two at every depth over 24 h, the diel fluctuations of phosphate were not as large. Phosphate concentrations temporarily increased after oxygenation, possibly

associated with increased mineralization of organic matter in the water column. Without additional data on the microbial and phytoplankton dynamics in the reservoir, we are unable to identify the mechanisms responsible for these diel cycles, but hypothesize that they may be due to a combination of internal waves as well as biological uptake and mineralization. We do not rule out, however, that the apparent diel fluctuations may result, in part, from an artifact of the co-variability between the color matrix, which may vary on a diel basis, and the elemental concentrations. Observing both large amplitude (e.g., for Fe and Si, $\geq 15\%$ change from diel minimum to maximum values) and small amplitude (e.g., for PO_4^{3-} ; $\leq 8\%$ change from diel minimum to maximum values) diel fluctuations does suggest, however, that these fluctuations cannot only result from a methodological artifact. Overall, these results highlight how dynamic freshwater biogeochemical cycles may be in lentic systems, as well as their sensitivity to changes in redox potential.

The coupled MPS-water quality probe system also elucidated some of the spatial variability of nitrate removal in constructed wetlands in the mesocosm experiment. The ability of the system to collect high-frequency (10-min) resolution data from each sediment site revealed the sensitivity of nitrate removal processes to water current velocity, as a result of increased advective exchange between the water column and the wetland sediment substrate. The positive response of nitrate removal to current velocity suggests that reported values in microcosms and mesocosm experiments for wetland, stream, lake and estuarine sediments in the literature (e.g., reviewed by Seitzinger 1988; Birgand et al. 2007) may not readily be comparable, as recirculation velocity is rarely taken into account or reported.

Finally, our high-frequency data also revealed that nitrate removal kinetics did not follow the traditionally accepted first order rate model: applying this traditional model to our data significantly underestimated nitrate removal efficiency. This conclusion would not have been possible without the coupled MPS-water quality probe system, which substantiated this observation in three different experiments and replicated mesocosms.

System limitations and opportunities

We note that the MPS-water quality probe system is flexible in deployment applications and could be coupled with any water quality probe collecting data at the minute scale, not just the S::CAN Spectro:lyserTM. In the applications we present here, it should be noted that the S::CAN probe could not be continuously deployed for more than 3 d before the memory of the instrument was full. In both mesocosm and reservoir applications, the probe saved > 200 absorbance values every 3 min, requiring data to be downloaded every third day. This limitation of the water quality probe should be quickly addressed by the manufacturer, however. The second limitation is the fouling of the optics or within the

cuvette. In the two applications shown, overlying water in the mesocosm experiment and hypolimnion in the reservoir was anoxic prior to pumping into the system. The sudden contact of reduced water with air in the cuvette created the conditions for metal oxidation, the precipitate of which partially coated the optics or the cuvette walls through time (Etheridge et al. 2013). These had to be cleaned regularly, at least every 24–72 h, using a 2% HCl solution. A third limitation is electrical power, which can be alleviated with the use of solar panel to recharge batteries.

Despite its imperfections, we believe that the coupled MPS-water quality probe system offers enormous potential and flexibility for the study of aquatic biogeochemical processes. The overall cost of materials for the MPS system presented in this article was less than \$2,500 USD in 2013 (not including the cost of the water quality probe or the time to assemble the parts). In sum, this system is very affordable for expanding the capabilities of one water quality probe to collect data at 12 sites, especially in comparison to purchasing 11 additional water quality probes. Most importantly, our system is well suited to capture processes linked in space and in time, especially the linkage between “hot spots” and “hot moments” (McClain et al. 2003; Vidon et al. 2010). As our understanding of biogeochemical hotspots and hot moments advances, we anticipate the deployment of similar systems across a diversity of ecosystems.

References

- Alexander, R. B., R. A. Smith, and G. E. Schwarz. 2000. Effect of stream channel size on the delivery of nitrogen to the Gulf of Mexico. *Nature* **403**: 758–761. doi:[10.1038/35001562](https://doi.org/10.1038/35001562)
- APHA, AWWA, and WEF (American Public Health Association, American Water Works Association, and Water Environment Federation). 1998. Standard methods for examination of water and wastewater, 20th ed. APHA.
- Basu, A. J., and A. Khalili. 1999. Computation of flow through a fluid-sediment interface in a benthic chamber. *Phys. Fluids* **11**: 1395–1405. doi:[10.1063/1.870004](https://doi.org/10.1063/1.870004)
- Bernot, M. J., and W. K. Dodds. 2005. Nitrogen retention, removal and saturation in lotic ecosystems. *Ecosystems* **8**: 442–453. doi:[10.1007/s10021-003-0143-y](https://doi.org/10.1007/s10021-003-0143-y)
- Birgand, F., R. W. Skaggs, G. M. Chescheir, and J. W. Gilliam. 2007. Nitrogen removal in streams of agricultural catchments—a literature review. *Crit. Rev. Environ. Sci. Technol.* **37**: 381–487. doi:[10.1080/10643380600966426](https://doi.org/10.1080/10643380600966426)
- Birgand, F., C. Faucheux, G. Gruau, B. Augeard, F. Moatar, and P. Bordenave. 2010. Uncertainties in assessing annual nitrate loads and concentration indicators: Part 1. Impact of sampling frequency and load estimation algorithms. *Trans. ASABE* **53**: 437–446. doi:[10.13031/2013.29584](https://doi.org/10.13031/2013.29584)
- Chapin, T. P., J. M. Caffrey, H. W. Jannasch, L. J. Colletti, J. C. Haskins, and K. S. Johnson. 2004. Nitrate sources and

- sinks in Elkhorn Slough, California: Results from long-term continuous in situ nitrate analyzers. *Estuaries* **27**: 882–894. doi:[10.1007/BF02912049](https://doi.org/10.1007/BF02912049)
- Cohen, M. J., J. B. Heffernan, A. Albertin, and J. B. Martin. 2012. Inference of riverine nitrogen processing from longitudinal and diel variation in dual nitrate isotopes. *J. Geophys. Res.* **117**: G01021. doi:[10.1029/2011JG001715](https://doi.org/10.1029/2011JG001715).
- Cohen, M. J., M. J. Kurz, J. B. Heffernan, J. B. Martin, R. L. Douglass, C. R. Foster, and R. G. Thomas. 2013. Diel phosphorus variation and the stoichiometry of ecosystem metabolism in a large spring-fed river. *Ecol. Monogr.* **83**: 155–176. doi:[10.1890/12-1497.1](https://doi.org/10.1890/12-1497.1)
- Crumpton, W. G., T. M. Isenhardt, and P. D. Mitchell. 1992. Nitrate and organic N analyses with second-derivative spectroscopy. *Limnol. Oceanogr.* **37**: 907–913. doi:[10.4319/lo.1992.37.4.0907](https://doi.org/10.4319/lo.1992.37.4.0907).
- Elliott, A. H., and N. H. Brooks. 1997. Transfer of nonsorbing solutes to a streambed with bed forms: Laboratory experiments. *Water Resour. Res.* **33**: 137–151. doi:[10.1029/96WR02783](https://doi.org/10.1029/96WR02783)
- Etheridge, J. R., F. Birgand, M. R. Burchell, II, and B. T. Smith. 2013. Addressing the fouling of in-situ UV-Visual spectrometers used to continuously monitor water quality in brackish tidal marsh waters. *J. Environ. Qual.* **42**: 1896–1901. doi:[10.2134/jeq2013.02.0049](https://doi.org/10.2134/jeq2013.02.0049)
- Etheridge, J. R., F. Birgand, J. A. Osborne, C. L. Osburn, M. R. Burchell, II, and J. Irving. 2014. Using in situ ultraviolet-visual spectroscopy to measure nitrogen, carbon, phosphorus, and suspended solids concentrations at a high frequency in a brackish tidal marsh. *Limnol. Oceanogr.: Methods* **12**: 10–22. doi:[10.4319/lom.2014.12.10](https://doi.org/10.4319/lom.2014.12.10)
- Gerling, A. B., R. G. Browne, P. A. Gantzer, M. H. Mobley, J. C. Little, and C. C. Carey. 2014. First report of the successful operation of a side stream supersaturation hypolimnetic oxygenation system in a eutrophic, shallow reservoir. *Water Res.* **67**: 129–143. doi:[10.1016/j.watres.2014.09.002](https://doi.org/10.1016/j.watres.2014.09.002)
- Gerling, A. B., Z. W. Munger, J. P. Doubek, K. D. Hamre, P. A. Gantzer, J. C. Little, and C. C. Carey. 2016. Whole-catchment manipulations of internal and external loading reveal the sensitivity of a century-old reservoir to hypoxia. *Ecosystems* **19**: 555–571. DOI:[10.1007/s10021-015-9951-0](https://doi.org/10.1007/s10021-015-9951-0)
- Hensley, R. T., M. J. Cohen, and L. V. Korhnak. 2015. Hydraulic effects on nitrogen removal in a tidal spring-fed river. *Water Resour. Res.* **51**: 1443–1456. doi:[10.1002/2014WR016178](https://doi.org/10.1002/2014WR016178)
- Horne, A. J. 1995. Nitrogen removal from waste treatment pond or activated sludge plant effluents with free-surface wetlands. *Water Sci. Technol.* **31**: 341–351. doi:[10.1016/0273-1223\(95\)00530-Z](https://doi.org/10.1016/0273-1223(95)00530-Z)
- Horstman, M. 2012. Wetland nitrate dissipation capacity enhancement via increased sediment interfacial nitrate transport. M.S. thesis. North Carolina State Univ.
- Huettel, M., W. Ziebis, and S. Forster. 1996. Flow-induced uptake of particulate matter in permeable sediments. *Limnol. Oceanogr.* **41**: 309–322. doi:[10.4319/lo.1996.41.2.0309](https://doi.org/10.4319/lo.1996.41.2.0309)
- Hutchinson, P. A., and I. T. Webster. 1998. Solute uptake in aquatic sediments due to current-obstacle interactions. *J. Environ. Eng.* **124**: 419–426. doi:[10.1061/\(ASCE\)0733-9372\(1998\)](https://doi.org/10.1061/(ASCE)0733-9372(1998))
- Kadlec, R. H., and S. D. Wallace. 2009. *Treatment wetlands*, 2nd ed, 182, 395, 472 p. CRC Press.
- Khalili, A., A. J. Basu, and M. Huettel. 1997. A non-Darcy model for recirculating flow through a fluid-sediment interface in a cylindrical container. *Acta Mech.* **123**: 75. doi:[10.1007/BF01178402](https://doi.org/10.1007/BF01178402)
- Khalili, A., A. J. Basu, U. Pietrzyk, and M. Raffel. 1999. An experimental study of recirculating flow through fluid-sediment interfaces. *J. Fluid Mech.* **383**: 229. doi:[10.1017/S0022112098003942](https://doi.org/10.1017/S0022112098003942)
- Marion, A., M. Bellinello, I. Guymer, and A. I. Packman. 2002. Effect of bed form geometry on the penetration of nonreactive solutes into a streambed. *Water Resour. Res.* **38**: W1209. doi:[10.1029/2001WR000264](https://doi.org/10.1029/2001WR000264)
- McClain, M. E., and others. 2003. Biogeochemical hot spots and hot moments at the interface of terrestrial and aquatic ecosystems. *Ecosystems* **6**: 301–312. doi:[10.1007/s10021-003-0161-9](https://doi.org/10.1007/s10021-003-0161-9)
- Mevik, B., R. Wehrens, and K. H. Liland. 2011. pls: Partial least squares and principal component regression. R package 2.3-0. Available from <http://CRAN.R-project.org/package=pls>. doi:[10.18637/jss.v018.i02](https://doi.org/10.18637/jss.v018.i02)
- Mitsch, W. J., J. W. Day, Jr., L. Zhang, and R. R. Lane. 2005. Nitrate-nitrogen retention by wetlands in the Mississippi River Basin. *Ecol. Eng.* **24**: 267–278. doi:[10.1016/j.ecoleng.2005.02.005](https://doi.org/10.1016/j.ecoleng.2005.02.005)
- Morsy, F. M. 2011. A simple approach to water and plankton sampling for water microbiological and physicochemical characterizations at various depths in aquatic ecosystems. *Int. J. Limnol.* **47**: 65–71. doi:[10.1051/limn/2010032](https://doi.org/10.1051/limn/2010032)
- Nimick, D. A., C. H. Gammons, and S. R. Parker. 2011. Diel biogeochemical processes and their effect on the aqueous chemistry of streams: A review. *Chem. Geol.* **283**: 3–17. doi:[10.1016/j.chemgeo.2010.08.017](https://doi.org/10.1016/j.chemgeo.2010.08.017)
- O'Brien, J. M., W. K. Dodds, K. C. Wilson, J. N. Murdock, and J. Eichmiller. 2007. The saturation of cycling in Central Plains streams: ¹⁵N experiments across a broad gradient of nitrate concentrations. *Biogeochemistry* **84**: 31–49. doi:[10.1007/s10533-007-9073-7](https://doi.org/10.1007/s10533-007-9073-7)
- Packman, A. I., and M. Salehin. 2003. Relative roles of stream flow and sedimentary conditions in controlling hyporheic exchange. *Hydrobiologia* **494**: 291–297. doi:[10.1023/A:1025403424063](https://doi.org/10.1023/A:1025403424063)
- Packman, A. I., M. Salehin, and M. Zaramella. 2004. Hyporheic exchange with gravel beds: Basic hydrodynamic interaction and bedform-induced advective flows. *J. Environ. Eng.* **130**: 647–656. doi:[10.1061/\(ASCE\)0733-9429\(2004\)](https://doi.org/10.1061/(ASCE)0733-9429(2004))

- Pellerin, B. A., and others. 2009. Assessing the sources and magnitude of diurnal nitrate variability in the San Joaquin River (California) with an in situ optical nitrate sensor and dual nitrate isotopes. *Freshw. Biol.* **54**: 376–387. doi:[10.1111/j.1365-2427.2008.02111.x](https://doi.org/10.1111/j.1365-2427.2008.02111.x)
- Pellerin, B. A., J. F. Saraceno, J. B. Shanley, S. D. Sebestyen, G. R. Aiken, W. M. Wollheim, and B. A. Bergamaschi. 2012. Taking the pulse of snowmelt: In situ sensors reveal seasonal, event and diurnal patterns of nitrate and dissolved organic matter variability in an upland forest stream. *Biogeochemistry* **108**: 183–198. doi:[10.1007/s10533-011-9589-8](https://doi.org/10.1007/s10533-011-9589-8)
- R Core Development Team. 2015. R: A language and environment for Statistical Computing. Available from <http://www.R-project.org>.
- Rieger, L., G. Langergraber, and H. Siegrist. 2006. Uncertainties of spectral in situ measurements in wastewater using different calibration approaches. *Water Sci. Technol.* **53**: 187–198. doi:[10.2166/wst.2006.421](https://doi.org/10.2166/wst.2006.421).
- Salehin, M., A. I. Packman, and A. Wörman. 2003. Comparison of transient storage in vegetated and unvegetated reaches of a small agricultural stream in Sweden: Seasonal variation and anthropogenic manipulation. *Adv. Water Res.* **26**: 951–964. doi:[10.1016/S0309-1708\(03\)00084-8](https://doi.org/10.1016/S0309-1708(03)00084-8)
- Savant, S. A., D. D. Reible, and L. J. Thibodeaux. 1987. Convective transport within stable river sediments. *Water Resour. Res.* **23**: 1763–1768. doi:[10.1029/WR023i009p01763](https://doi.org/10.1029/WR023i009p01763)
- S::CAN Spectrometer Probe V2. 2011. User Manual. Vienna, Austria.
- Seitzinger, S. P. 1988. Denitrification in freshwater and coastal marine ecosystems: Ecological and geochemical significance. *Limnol. Oceanogr.* **33**: 702–724. doi:[10.4319/lo.1988.33.4part2.0702](https://doi.org/10.4319/lo.1988.33.4part2.0702)
- Singleton, V. L., and J. C. Little. 2006. Designing hypolimnetic aeration and oxygenation systems: A review. *Environ. Sci. Technol.* **40**: 7512e–7520. doi:[10.1021/es060069s](https://doi.org/10.1021/es060069s)
- Smith, R. A., G. E. Schwarz, and R. B. Alexander. 1997. Regional interpretation of water-quality monitoring data. *Water Resour. Res.* **33**: 2781–2798. doi:[10.1029/97WR02171](https://doi.org/10.1029/97WR02171)
- Snyder, L., and W. B. Bowden. 2014. Nutrient dynamics in an oligotrophic arctic stream monitored in situ by wet chemistry methods. *Water Resour. Res.* **50**: 2039–2049. doi:[10.1002/2013WR014317](https://doi.org/10.1002/2013WR014317)
- Stream Solute Workshop. 1990. Concepts and methods for assessing solute dynamics in stream ecosystems. *J. N. Am. Benthol. Soc.* **9**: 95–119. doi:[10.2307/1467445](https://doi.org/10.2307/1467445)
- Suzuki, N., and R. Kuroda. 1987. Direct simultaneous determination of nitrate and nitrite by ultraviolet second-derivative spectrophotometry. *Analyst* **112**: 1077–1079. doi:[10.1039/an9871201077](https://doi.org/10.1039/an9871201077)
- Thibodeaux, L. J., and J. O. Boyle. 1987. Bed-form generated convective transport in bottom sediment. *Nature* **325**: 341–343. doi:[10.1038/325341a0](https://doi.org/10.1038/325341a0)
- Torres, A., and J. L. Bertrand-Krajewski. 2008. Partial Least Squares local calibration of a UV-visible spectrometer used for in situ measurements of COD and TSS concentrations in urban drainage systems. *Water Sci. Technol.* **57**: 581–588. doi:[10.2166/wst.2008.131](https://doi.org/10.2166/wst.2008.131).
- Vidon, P., and others. 2010. Hot spots and hot moments in riparian zones: Potential for improved water quality management. *J. Am. Water Resour. Assoc.* **46**: 278–298. doi:[10.1111/j.1752-1688.2010.00420.x](https://doi.org/10.1111/j.1752-1688.2010.00420.x)
- Watras, C. J., K. A. Morrison, J. T. Crawford, C. P. McDonald, S. K. Oliver, and P. C. Hanson. 2015. Diel cycles in the fluorescence of dissolved organic matter in dystrophic Wisconsin seepage lakes: Implications for carbon turnover. *Limnol. Oceanogr.* **60**: 482–496. doi:[10.1002/lno.10026](https://doi.org/10.1002/lno.10026)
- Watras, C. J., K. A. Morrison, N. R. Lottig, and T. K. Kratz. 2016. Comparing the diel cycles of dissolved organic matter fluorescence in a clear-water and two dark-water Wisconsin lakes: Potential insights into lake metabolism. *Can. J. Fish. Aquat. Sci.* **73**: 65–75. doi:[10.1139/cjfas-2015-0172](https://doi.org/10.1139/cjfas-2015-0172)
- YSI Environmental. 2006a. Monitoring and Protecting Water Quality in Lake Mead, Nevada. Application note 0506 A539.
- YSI Environmental. 2006b. Monitoring the Water Quality of Lake Olathe and Protecting Drinking Water for Olathe Residents. Application note 0306 A538.

Acknowledgments

We thank C. Garland and R. Perry for the early design and for assembling the first prototype of the MPS system; J. P. Doubek, K. D. Hamre, Z. W. Munger, and R. Q. Thomas for assistance in the field, and the Western Virginia Water Authority for access to field sites. This work was financially supported by North Carolina State University, National Institute of Food and Agriculture multistate project S1063, and the Virginia Tech Institute of Critical Technology and Applied Science, Western Virginia Water Authority, and Fralin Life Science Institute.

Submitted 13 January 2016

Revised 22 April 2016

Accepted 14 June 2016

Associate editor: Clare Reimers